SUPPLEMENTAL FIGURES

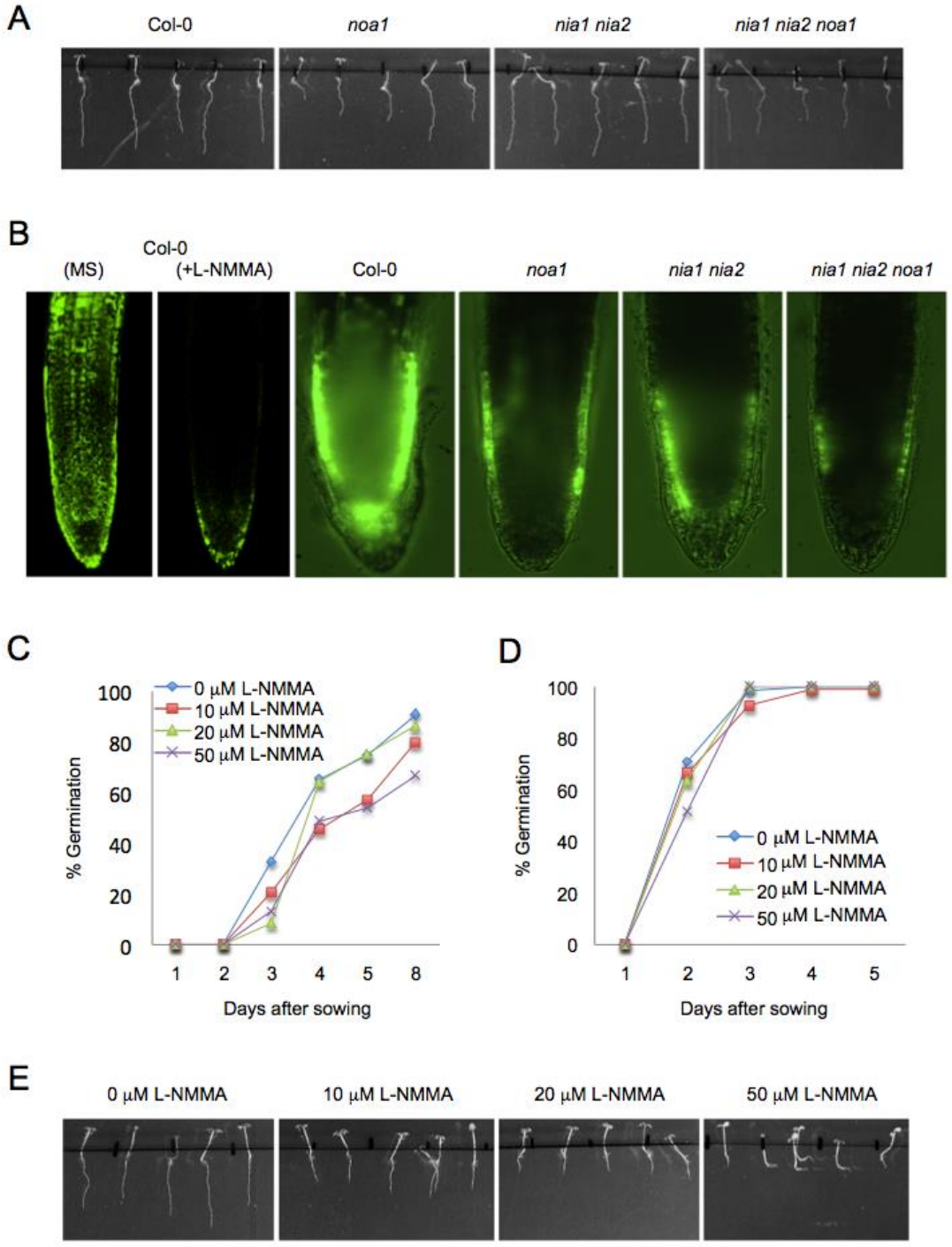

Figure S1. Genetic and pharmacological effect of NO depletion on primary root growth. A, Picture showing the longitudinal primary root growth of Col-0, *noa1*, *nia1 nia2* and *nia1 nia2 noa1* seedlings grown vertically for 7 days under standard conditions. B, Detection of endogenous NO production using DAF-2DA in roots of 5-day-old wild type (Col-0) seedlings grown in the presence or absence of 20 μM L-NMMA and *noa1*, *nia1 nia2* and *nia1 nia2 noa1* mutants. C, Dose response (0, 10, 20 and 50 μM) analysis of

the effect of NO synthase inhibitor L-NMMA of Col-0 seeds two weeks after harvest (non-stratified). D, Dose response (0, 10, 20 and 50 μM) analysis of the effect of L-NMMA of Col-0 seeds two weeks after harvest following 48 h of cold treatment at 4°C to remove dormancy (stratified). E, Picture showing the longitudinal primary root growth of Col-0 seedlings grown vertically for 7 days in the presence of 0, 10, 20 and 50 μM L-NMMA.

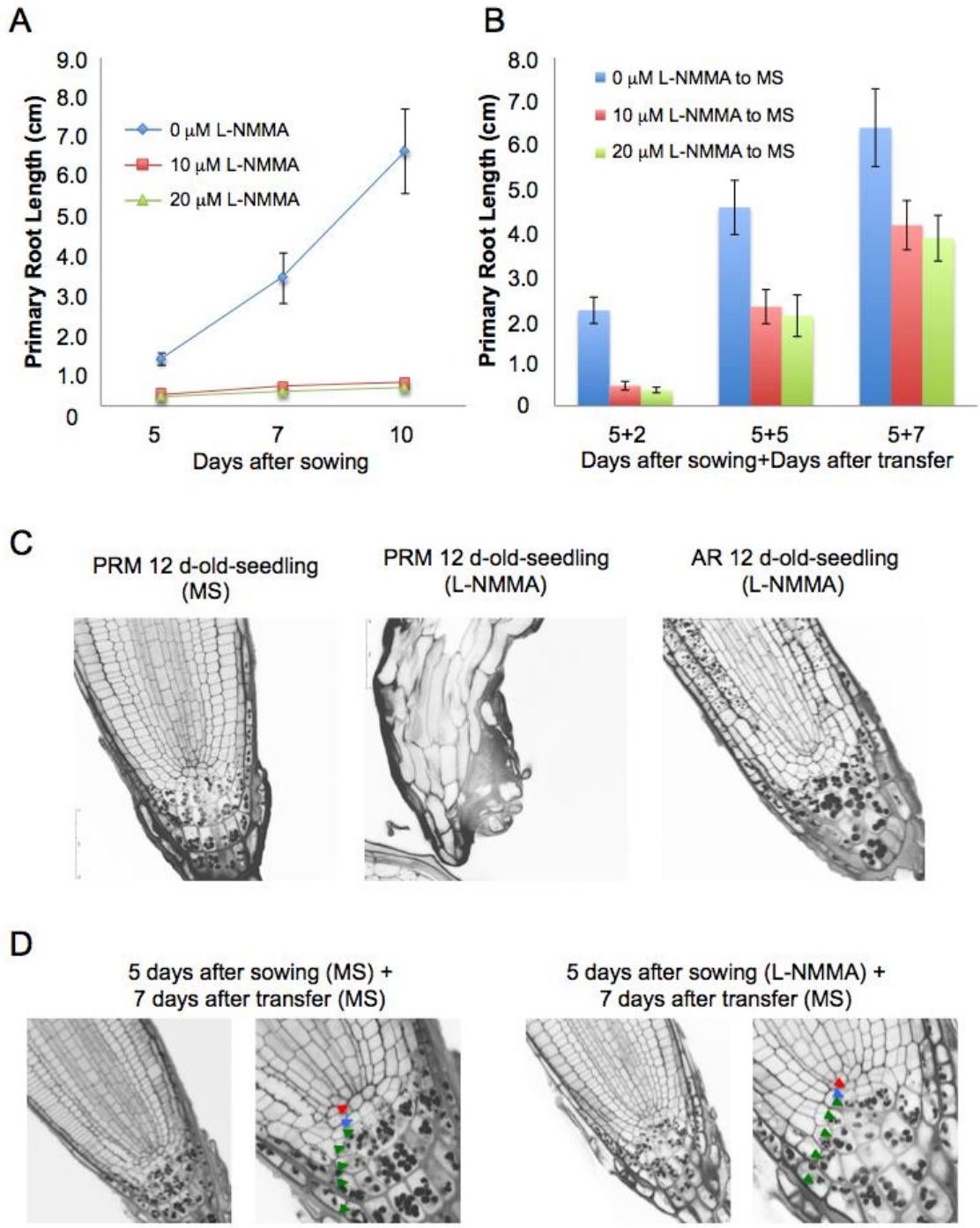

Figure S2. Effect of L-NMMA on primary root growth. A, Time course (from 5 to 10 days after sowing) of longitudinal primary root growth of Col-0 seedlings grown vertically in the presence of 0, 10 and 20 μM L-NMMA (+DMSO). Error bars represent SE; n>40. B, Time course of longitudinal primary root growth of Col-0 seedlings grown vertically in the presence of 0, 10 and 20 μM L-NMMA (+DMSO) for 5 days and then transferred during 2, 5 or 7 days to plates containing MS media. Error bars represent SE; n>40. C, Meristematic regions of 12-day-old wild type (Col-0) primary roots (PRM) and adventitious roots (AR) grown in the presence or absence of 20 μM L-NMMA. D,

Meristematic regions of 12-day-old wild type (Col-0) roots grown in the presence or absence of 10 μM L-NMMA (+DMSO) for 5 days and then transferred during 7 days to plates containing MS media. QC/CSC disorganization and starch accumulation by using modified pseudo-Schiff propidium iodide (mPS-PI)-stained. Red, blue and green arrowheads indicate QC, CSC and columella cells, respectively.

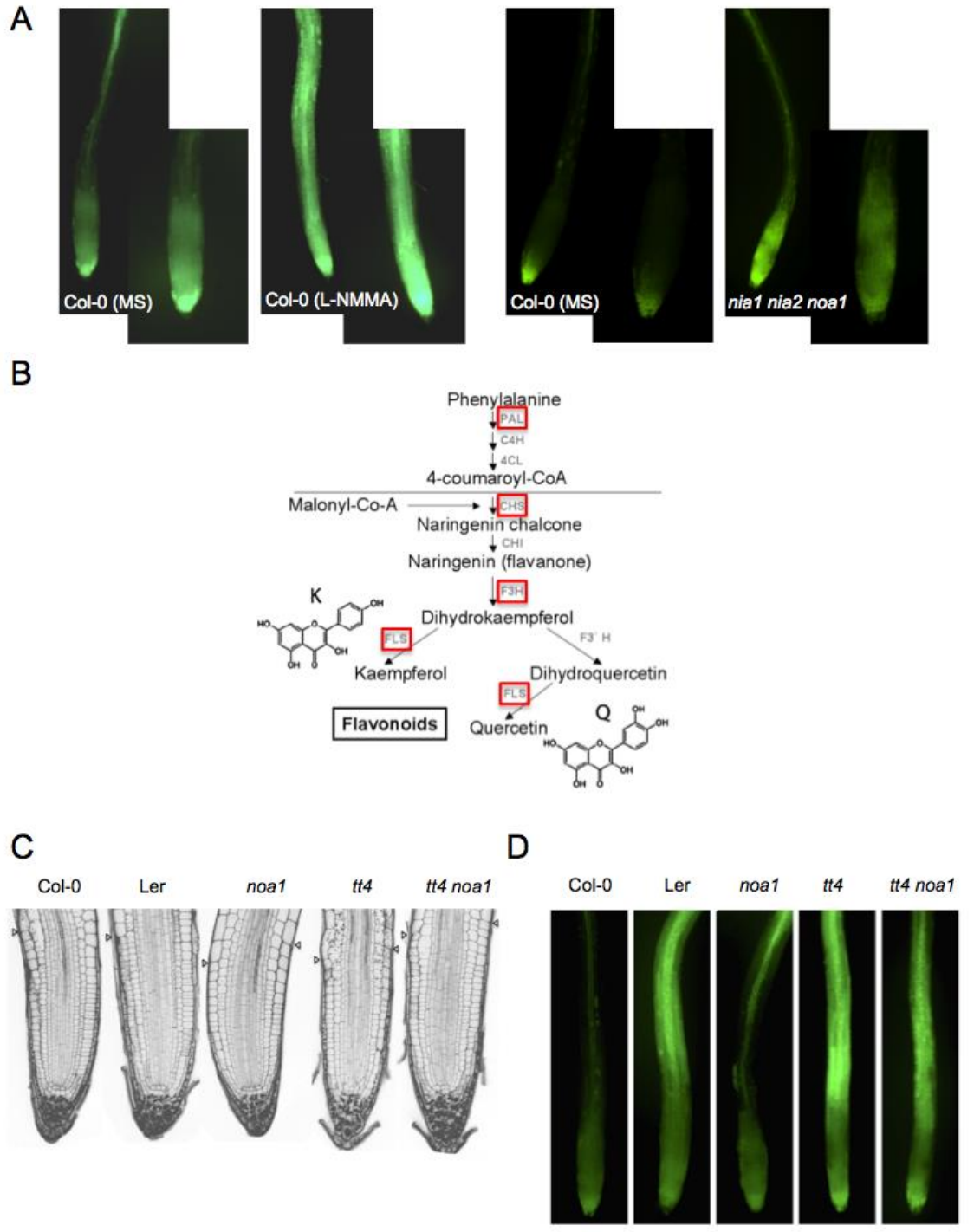

Figure S3. Contribution of flavonol and ROS accumulation to the NO-deficient mutant phenotype. A, ROS accumulation in roots of 5-day-old wild type (Col-0) seedlings grown in the presence or absence of 20 μM L-NMMA and *nia1 nia2 noa1* mutants. B, Intermediate compounds and enzymes in the flavonoid biosynthetic pathway are shown. The structures of kaempferol and quercetin and upstream metabolites are represented in the diagram. Enzymes central to this study are shown in red squares.

This figure is modified from Buer and Muday (2004). C, Meristematic regions of 5-day-old Col-0, Ler, *noa1*, *tt4* and *tt4 noa1* roots grown vertically under standard conditions. Arrows indicate the end of the meristem and the beginning of the elongation-differentiation zone. D, ROS accumulation in roots of 5-day-old wild type (Col-0, Ler) seedlings and *noa1*, *tt4* and *tt4 noa1* mutants.

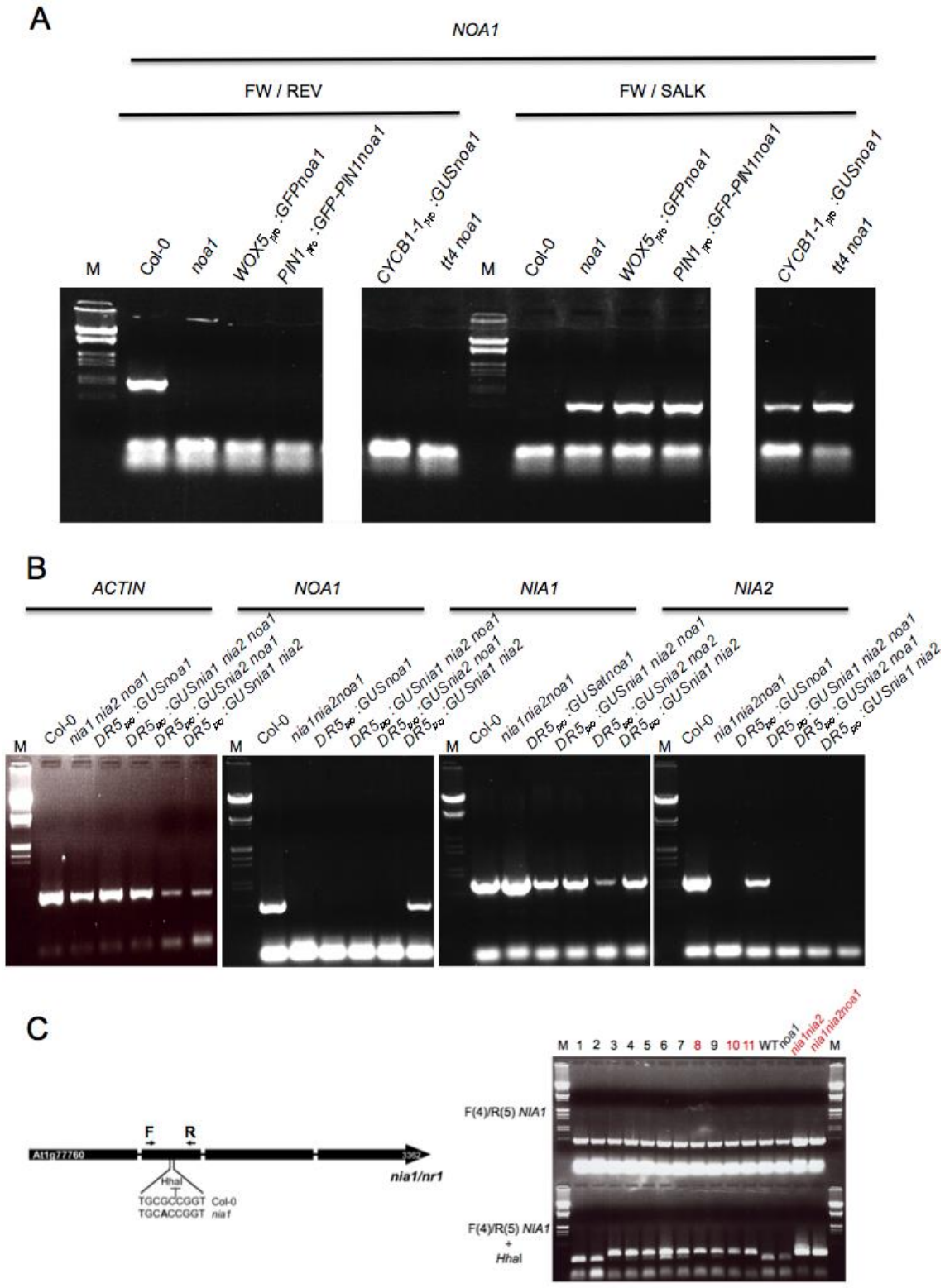

Figure S4. Genetic characterization of *noa1*-based double mutants and reporter lines under NO-deficient mutant backgrounds. A, PCR-based genotyping to evaluate T-DNA insertion in *NOA1* gene in wild type (Col-0), *noa1*, *WOX5*$_{pro}$*:GFPnoa1*, *PIN1*$_{pro}$*:GFP-PIN1noa1*, *CycB1;1*$_{pro}$*:GUSDBnoa1* and *tt4 noa1* seedlings. Ethidium bromide-stained

amplicons of different combinations of primers are shown. B, RT-PCR-based analysis of *NOA1*, *NIA1* and *NIA2* transcripts in wild type (Col-0), *nia1 nia2 noa1*, *DR5*$_{pro}$*:GUSnoa1*, *DR5*$_{pro}$*:GUSnia1 nia2 noa1*, *DR5*$_{pro}$*:GUSnia2 noa1* and *DR5*$_{pro}$*:GUSnia1 nia2* seedlings. Total RNAs from the indicated genotypes were extracted from 10-d-old seedlings, treated with DNase, reverse transcribed, and separated on 1% agarose gels. *ACTIN8* expression was used as a loading control. C, Genotyping of *nia1* mutation in selected F2 plants by Cleaved Amplified Polymorphic Sequences (CAPS) polymorphisms between mutant and wild type and digestion with *Hha*I restriction endonuclease. Plants 8, 10 and 11 resulted homozygous for the *nia1* mutation (red). Diagram on the left is modified from Lozano-Juste and León (2010).

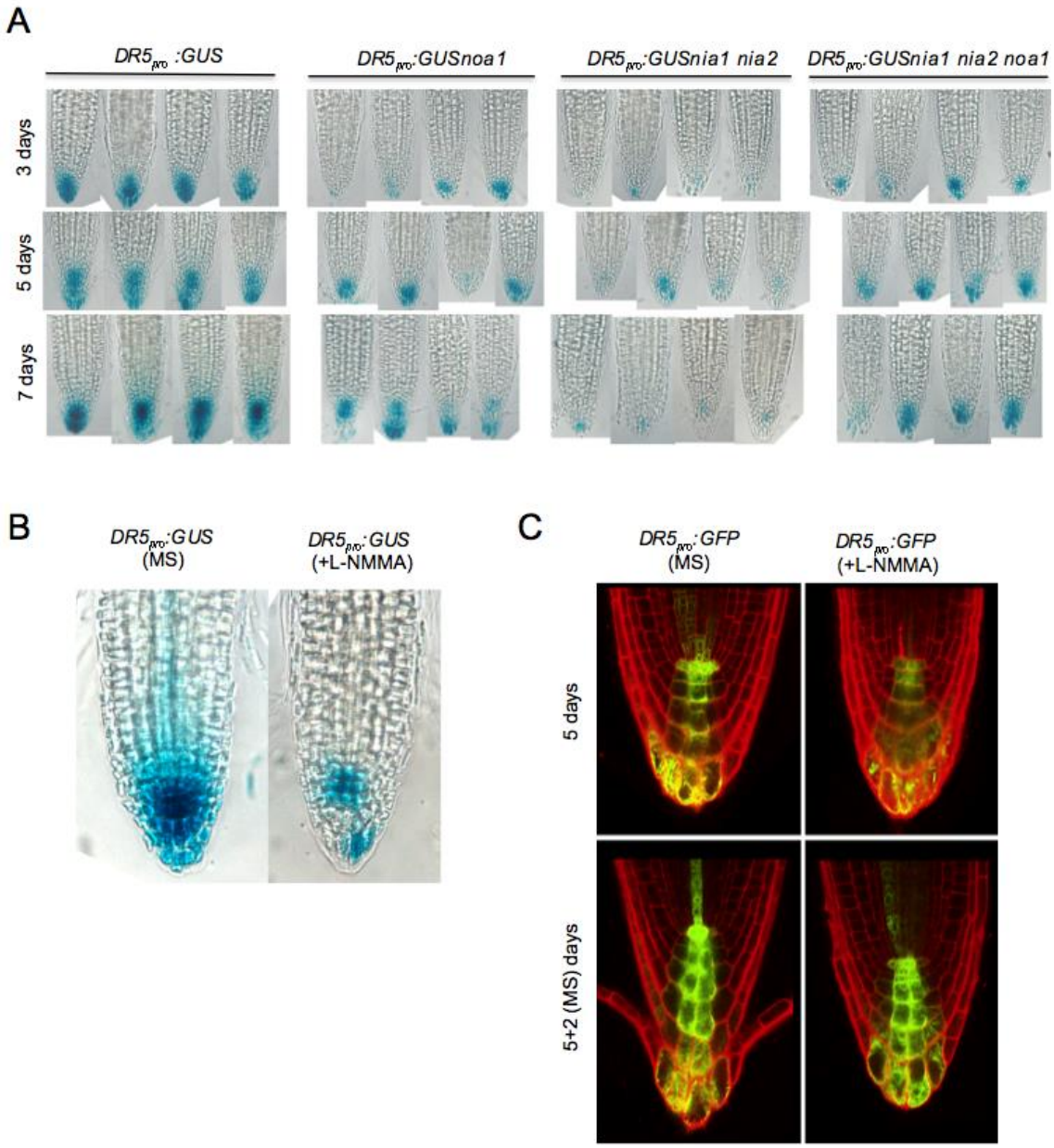

Figure S5. Effect of NO depletion on auxin signalling in the primary root. A, GUS-stained *DR5$_{pro}$:GUS*-expressing wild type (Col-0), *noa1, nia1 nia2* and *nia1 nia2 noa1* mutant roots 3, 5 and 7 days after sowing. B, *DR5* marker analysis in 5 day-old wild type seedlings grown in media containing 20 μM L-NMMA. C, *DR5$_{pro}$:GFP* marker analysis in 5 day-old wild type seedlings grown in media containing 20 μM L-NMMA and after recovery 2 days in MS media.

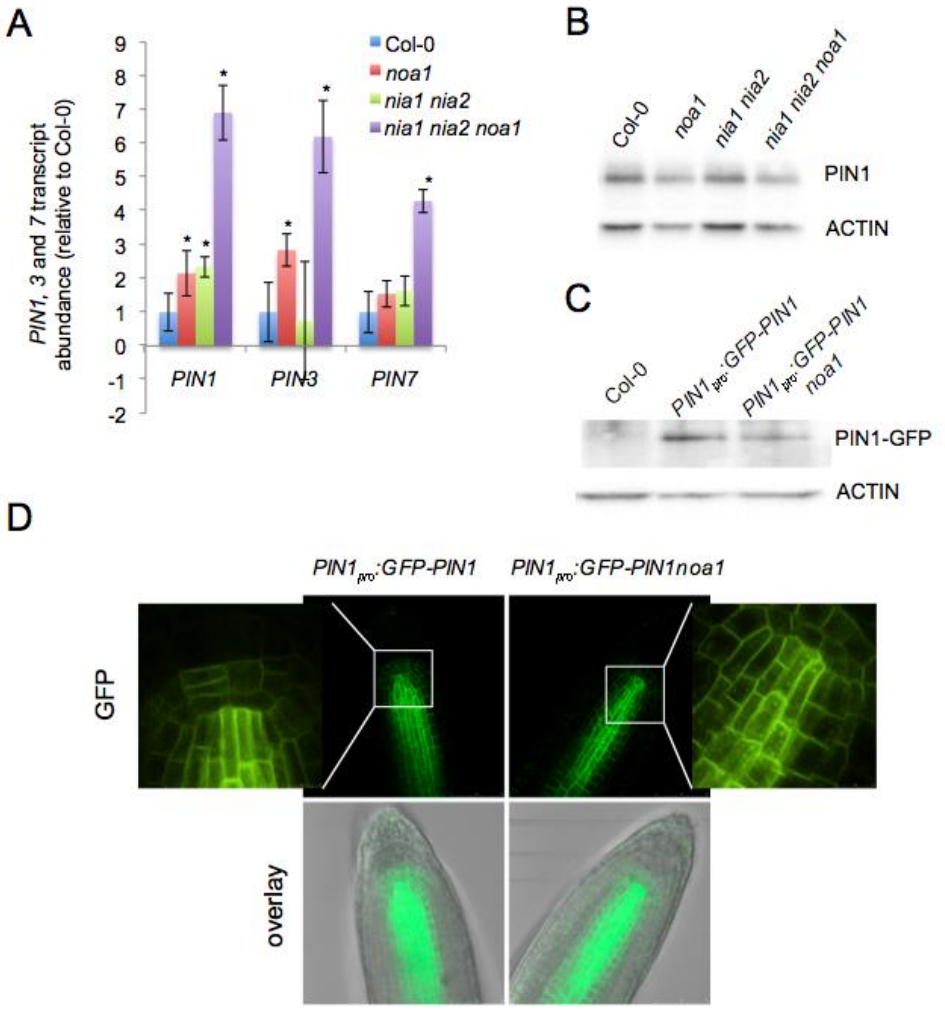

Figure S6. Effect of NO-deficient mutants on *PIN1* transcript and protein accumulation. A, *PIN1, PIN3 and PIN7* transcription levels in roots of wild type (Col-0) and *noa1*, *nia1 nia2* and *nia1 nia2 noa1* mutants. Asterisk indicates a statistically significant difference from the wild type ($P<0.05$). B, Immunoblot analysis with anti-PIN1 antiserum of *in vivo* levels of PIN1 protein in root extracts of wild type (Col-0), *noa1*, *nia1 nia2* and *nia1 nia2 noa1* 7-day-old-seedlings. Actin protein levels were determined as a loading control. C, Protein gel blot analysis using anti-GFP antiserum of root extracts from the untransformed wild type (Col-0), *PIN1$_{pro}$:GFP-PIN1* and *PIN1$_{pro}$:GFP-PIN1noa1* lines. Actin protein levels were determined as a loading control. D, *PIN1$_{pro}$:GFP-PIN1* expression in wild type and *noa1* mutant.

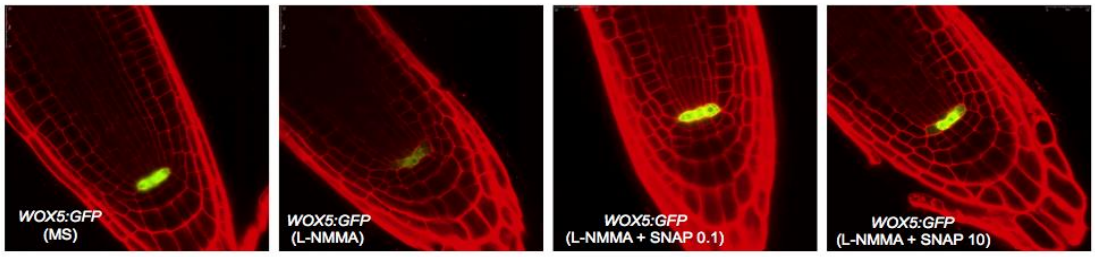

Figure S7. *WOX5* marker analysis in 5 day-old wild type (Col-0) roots grown in the absence (MS), presence of 20 µM L-NMMA and in media containing 20 µM L-NMMA plus the addition of SNAP (0.1 and 10 µM).

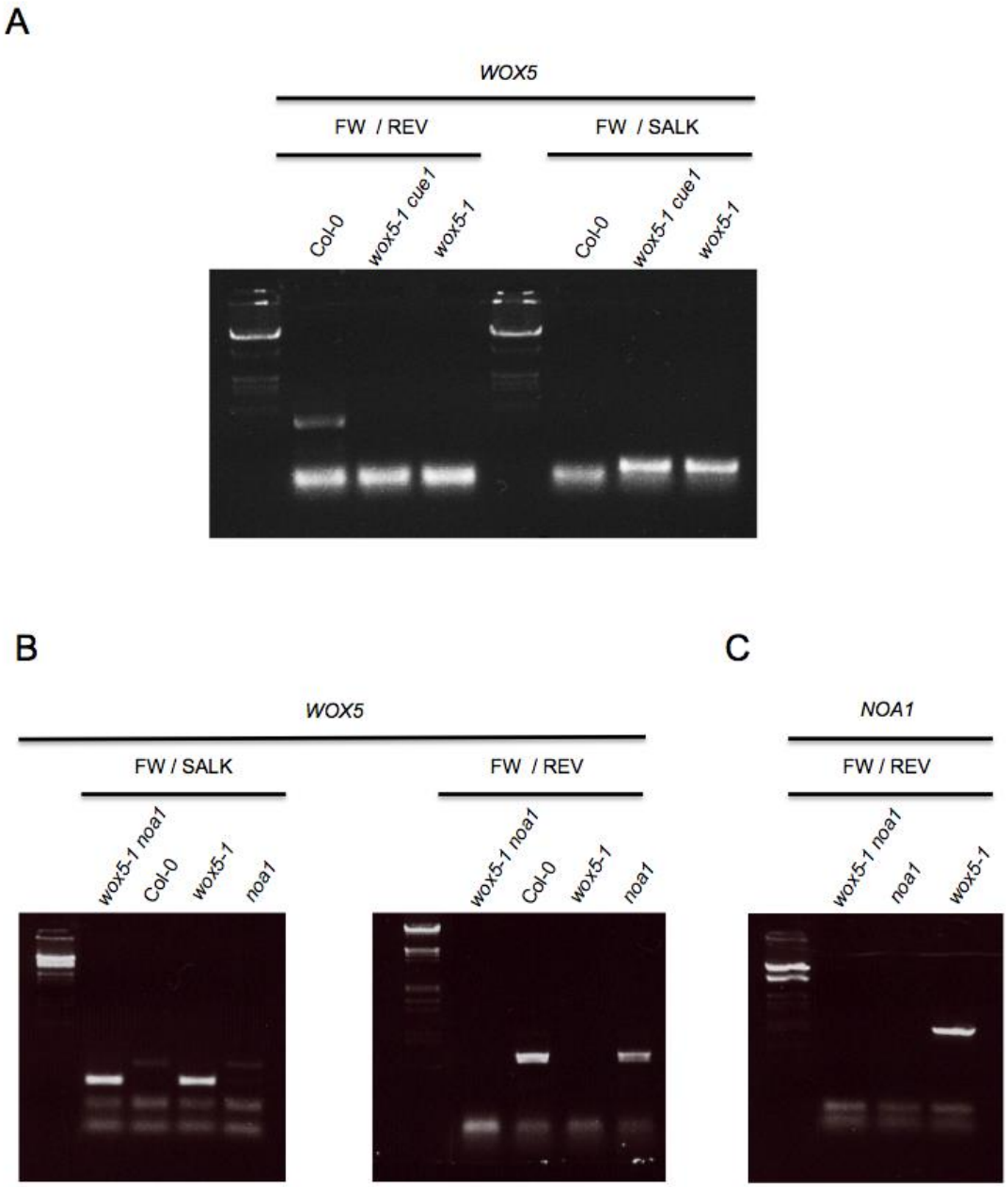

Figure S8. Genetic characterization of *wox5*-based double mutants and reporter lines. A, PCR-based genotyping to evaluate T-DNA insertion in *WOX5* gene in wild type (Col-0), *wox5-1*, *cue1* and *wox5-1 cue1* seedlings. Ethidium bromide-stained amplicons of different combinations of primers are shown. B, PCR-based genotyping to evaluate T-DNA insertion in *WOX5* gene in wild type (Col-0), *wox5-1*, *noa1* and *wox5-1 noa1* seedlings. Ethidium bromide-stained amplicons of different combinations of primers are shown. C, PCR-based genotyping to evaluate T-DNA insertion in *NOA1* gene in wild type (Col-0), *wox5-1*, *noa1* and *wox5-1 noa1* seedlings. Ethidium bromide-stained amplicons of different combinations of primers are shown.

SUPPLEMENTAL TABLES

Table S1. Concentration of individual flavonols (mg/g dry weight)* in Col-0 wild type seedlings and NO-deficient mutants *nia1 nia2* and *noa1*.

Compound	Col-0	*noa1*	*nia1 nia2*
Quercetin 3-O-rhamnosylglucoside7-O-rhamnoside	0.117±0.013[a]	0.388±0.036[c]	0.286±0.005[b]
Quercetin 3-O- rhamnoside 7-O-glucoside	0.165±0.045[a]	0.301±0.008[b]	0.303±0.011[b]
Kaempferol 3-O-rhamnoside 7-O-glucoside	0.208±0.057[a]	0.560±0.023[b]	0.394±0.021[b]

* For each compound concentration was expressed as aglycone equivalents ± SD (n=3).
[a,b] Different letters in a row mean significant differences (P<0.05); nd = not detected; nq = not quantifiable.

Table S2. Total flavonol concentration (mg/g dry weight)* in Col-0 wild type seedlings and NO-deficient mutants *nia1 nia2* and *noa1*.

Compound	Col-0	*noa1*	*nia1 nia2*
Kaempferol glycosides	0,429±0,118[a]	1,223±0,061[b]	0,988±0,114[b]
Quercetin glycosides	0,353±0,075[a]	0,852±0,064[b]	0,728±0,038[b]
Isorhamentin glycosides	0.050±0.009[a]	0.082±0.009[ab]	0.102±0.003[b]
Total flavonols	**0.832±0.022[a]**	**2.157±0.133[b]**	**1.819±0.159[b]**

Quercetin 3-O-rhamnoside 7-O-rhamnoside	0.071±0.017[a]	0.164±0.020[b]	0.139±0.004[b]
Isorhamnetin 3-O-rhamnoside 7-O-glucoside	0.050±0.009[a]	0.082±0.009[ab]	0.102±0.003[b]
Kaempferol 3-O-rhamnoside-7-O-rhamnoside	0.222±0.062[a]	0.663±0.038[b]	0.594±0.036[b]
Quercetin 3-O-rhamnoside	nd	nd	nd
Kaempferol 3-O-rhamnoside	nd	nq	nd

* Concentration expressed as aglycone equivalents ± SD (n=3).

[a,b] Different letters in a row mean significant differences (P<0.05)

Table S3. Pseudomolecular and MS^2 product ions of the analysed flavonols.

Compound	Pseudomolecular ion $[M-H]^-$ (*m/z*)	MS^2 (*m/z*)
Quercetin 3-*O*-rhamnosylglucoside 7-*O*-rhamnoside	755	609, 447, 301
Quercetin 3-*O*-rhamnoside 7-*O*-glucoside	609	447, 301
Kaempferol 3-*O*-rhamnoside 7-*O*-glucoside	593	447, 285
Quercetin 3-*O*-rhamnoside 7-*O*-rhamnoside	593	447, 301
Isorhamnetin 3-*O*-rhamnoside 7-*O*-glucoside	623	477, 315
Kaempferol 3-*O*-rhamnoside-7-*O*-rhamnoside	577	431, 285
Quercetin 3-*O*-rhamnoside	447	301
Kaempferol 3-*O*-rhamnoside	431	285

Table S4. List of primers used in the Q RT-PCR analysis and mutant genetic characterization.

F3H
Forward: 5' TGCACTTGTCTATGACAAAAACATC 3'
Reverse: 5' ACATAAACCCAACGCGTCA 3'
FLS1
Forward: 5' TCACATCGGCGATCAGATT 3'
Reverse: 5' GGGAGGCTCCAAGAAAACC 3'
FLS3
Forward: 5' TCAATCACAAATTCTGGCCTAA 3'
Reverse: 5' TGCGTACTCTTCATTCACTTCAA 3'
CHS
Forward: 5' TCAGGCGGAGTATCCTGACTA 3'

Reverse: 5' CGTTTCCGAATTGTCGACTT 3’
PAL
Forward: 5' ATTAACGGGGCACACAAGAG 3’
Reverse: 5' GTCTCCGCCGCATAACATAG 3’
WOX5
Forward: 5' CTATTGGTTTCAGAATCATAAGGCTA 3'
Reverse: 5' TGACAATCTTCTTCGCTTATTTCA 3'
PIN1
Forward: 5' CCTCAGGGGAATAGTAACGACA 3'
Reverse: 5' TCATCGTCTTTGTTACCGAAACT 3'
PIN3
Forward: 5' CCCAGATCAATCTCACAACG 3'
Reverse: 5' CCGGCGAAACTAAATTGTTG 3'
PIN7
Forward: 5' TGGGCTCTTGTTGCTTTCA 3'
Reverse: 5' TCACCCAAACTGAACATTGC 3'
ACTIN8
Forward: 5' AGTGGTCGTACAACCGGTATTGT 3'
Reverse: 5' GAGGATAGCATGTGGAAGTGAGAA 3'

LB SALK T-DNA
Forward: 5' GCGTGGACCGCTTGCTGCAACT 3'

***noa1-1* IDENTIFICATION**
Forward: 5' CCTGCAACACAACAAGTTGACG 3'
Reverse: 5' GGGCGGATATAACCGTCTCCA 3'

***wox5-1* IDENTIFICATION**
Forward: 5' ATGTCTTTCTCCGTGAAAGGTGG 3'
Reverse: 5' CGAAGATCTAATGGCGGTGG 3'

***noa1-2* IDENTIFICATION**
Forward: 5' GCACCTACACCACAGGCAAGC 3'
Reverse: 5' CCAATTGGCAATGTTGGTCG 3'

***nia1* IDENTIFICATION**
Forward: 5' TACGACGACTCCTCAAGCGAC 3'
Reverse: 5' GGCTATAGATCCCGCATCGAC 3'

***nia2* IDENTIFICATION**
Forward: 5' ACGGCGTGGTTCGTTCTTACA 3'
Reverse: 5' ACCTTCTTCGTCGGCGAGTTC 3'